# Shifts in the gut microbiota structure caused by *Helicobacter pylori* eradication therapy

Evgenii I. Olekhnovich[1*], Alexander I. Manolov[1], Nikita A. Prianichniikov[1], Andrei E. Samoilov[1], Maja V. Malakhova[1], Alexander V. Pavlenko[1], Vlad V. Babenko[1], Andrei K. Larin[1], Yuriy Y. Babin[1], Elizaveta V. Starikova[1], Dmitry I. Chuvelev[1], Boris A. Kovarsky[1], Maria A. Tregubova[1], Dilyara D. Safina[3], Maria I. Markelova[3], Tatiana V. Grigoryeva[3], Sergey Yu. Malanin[3], Rustam A. Abdulkhakov[2], Sayar R. Abdulkhakov[2,3], Elena S. Kostryukova[1], Elena N. Ilina[1] and Vadim M. Govorun[1].

*Corresponding author
Contact e-mail: olekhnovich@rcpcm.org

[1]Federal Research and Clinical Centre of Physical-Chemical Medicine, Malaya Pirogovskaya 1a, Moscow 119435, Russia
[2]Kazan State Medical University, 49 Butlerova, Kazan, 420012, Russia
[3] Kazan Federal University, 18 Kremlyovskaya, Kazan, 420008, Russia

**Abstract**

The human gut microbiome plays an important role both in health and disease. The use of antibiotics can alter gut microbiota composition, which can cause complications of various kinds. Here we report a whole-genome sequencing metagenomic study of the intestinal microbiota changes caused by *Helicobacter pylori* eradication therapy. We have found the significant decrease in taxonomic alpha-diversity due to the therapy. The changes observed were more extensive for patients with duodenal ulcer and female ones. We also observed perturbations in intraspecies structures ("strains"), which were significantly higher in group of patients under the therapy than in control group of people without treatment. As well across the patients under the *H. pylory* eradication therapy we have detected the shifts in the metabolic potentials and resistome. Metabolic pathways associated with the metabolism of carbohydrates and chorismate decreased. Changes in the resistome profile have also been identified: antibiotic resistance genes (ARGs) to macrolides were increased and to tetracyclines - decreased. We also isolated and sequenced *Enterococcus faecium* strains from two patients. After the therapy this bacterium increased antibiotic resistance in vitro, it had higher ARGs to macrolides and tetracyclines, and this bacterium relative abundance in metagenome was at higher level in comparison with strains before therapy.

## Introduction

*Helicobacter pylori* are ubiquitous bacteria classified by WHO as a cancer risk factor. It has been estimated that up to 50% of human population harbor this pathogen. It is supposed that *H. pylori* colonized the human stomach about 60 000 years ago after humanity's ancestors migrated from Eastern Africa. Currently, *H. pylori* infection is associated with wide range of gastrointestinal diseases, including chronic gastritis, stomach ulcer, duodenal ulcer, gastric cancer, lymphoma of mucin-associated lymphoid tissue (Sanders et al., 2002). This bacterium is also responsible for iron-deficiency anemia, Werlhof disease in children

(Queiroz et al., 2013), nutritional anemia due to vitamin $B_{12}$ deficiency, thrombocytopenic purpura, lipid, and glucose metabolism disorders (Buzás, 2014).

Conventional *H. pylori* eradication therapy regimens are based on antibiotics (clarithromycin, amoxicillin, tetracycline, metronidazole), proton pump inhibitors and some other auxiliary drugs treatment, including bismuth salts (Malfertheiner et al., 2016). It is known that antibiotic treatment can significantly alter gut microbial community composition, and, as the result, may cause such complications as antibiotic-associated diarrhea (Bartlett et al., 2002; Tong et al., 2007). Bacteria can acquire antibiotic resistance by a number of ways that are associated either with single-nucleotide polymorphisms (SNPs) in antibiotic-target sites or with the exchange of the genes encoding efflux pumps, drug modifiers or proteins which protect antibiotic targets (Wright 2007; Davies and Davies 2010). Antibiotic resistance genes (ARGs) may be transferred among the bacteria by mobile genetic elements, bacteriophages and also as the result of natural transformation (Davies and Davies 2010; Schjørring and Krogfeldt 2011; Smillie et al. 2011). The term “resistome” has been coined to refer to the collection of antibiotic resistance genes in a certain microbial community (Wright 2007; Marshall and Levy 2011). Resistome of human gut microbiota differs widely among the people of different countries and reflects peculiarities of antibiotic use (Forslund et al., 2013; Yarygin et al., 2017). Eradication therapy regimes include proton-pump inhibitors treatment which may lead to a significant shift in the gut microbial community due to the intrusion by the species that under normal conditions can’t pass gastric acid barrier (Jackson et al., 2016; Imhann et al., 2016).

Thus, eradication therapy can have a great impact on the gut microbial community composition. Among the drugs which are used during *H.pylori* treatment antibiotics are of great interest as they cause changes in the microbial community at the taxonomic and functional levels. These changes can drive gut disorders and cause accumulation of antibiotics resistance genes in the gut microbial community. Here we used whole-genome shotgun sequencing (WGS) to study taxonomic and functional profile shifts of the gut microbial community in the patients after *H. pylori* eradication therapy. Our research may contribute to better understanding of the processes in the gut microbiota, which are driven by the complex mix of drugs used during *H. pylori* eradication therapy.

## Materials and methods

### *Sample collection*

Faecal samples were collected prior to and following eradication therapy from the patients showing clinical signs of the diseases associated with *H. pylori* infection (gastroesophageal reflux disease, chronic gastritis, chronic duodenitis, and duodenal ulcer). For *H. pylori* detection, mucosal biopsies were collected from the antral part of the stomach during gastroscopy study. Specific bacterial cells availability was confirmed in the bioptates by the urease test and cytological examination. All the patients included in the study were going to have *H. pylori* eradication treatment. Summary information on the diagnosis of the patients is shown in the Supplementary Table S1.

Some patients were excluded from the sample due to the additional criteria which may influence microbial community (see Supplementary Note S1). Two sampling points were included: before the treatment and 0 or 2 days after the treatment. A total of 80

samples from 40 patients were collected (47.7±13.11 years old, 18 female and 22 male). Before the start of the study, each patient signed an informed consent.

***Helicobacter pylori eradication therapy scheme***

The eradication therapy was carried out according to the Maastricht scheme (Malfertheiner et al., 2016), which included amoxicillin 1000 mg, clarithromycin 500 mg, bismuth subsalicylate 240 mg, proton pump inhibitor (esomeprazole/pantoprazole) 20 mg. The therapy course lasted for 14 days. Lactulose was used as a prebiotic throughout the therapy course.

***Sample preparation and sequencing***

Stool samples were delivered to the laboratory in a frozen state and subsequently were stored at - 20 °C. Before the DNA extraction procedure, the aggregate state of the samples was evaluated and their weight was determined. The weight of all the samples exceeded 20 grams, which was a sufficient quantity for the extraction of the required amount of DNA. Total DNA extraction was performed as described previously (Tyakht et al., 2013). The whole genome shotgun sequencing on SOLiD 5500W platform in the 50 base pairs in single-end mode was performed according to the manufacturer's recommendations (Life Technologies, Foster City, CA, USA) using the following kits: 5500W Conversion Primers Kit, 5500 W FlowChip V2, 5500 W FlowChip Prep Pack, 5500W Template Amplification Kit v2, 5500 W FWD1 SP Kit, Double, 5500W FWD2 SP Kit, Double, 5500W FWD SR Kit, Double, 5500W FWD Ligase Kit, Double, 5500W Run Cycle Buffer Kit, 5500W FWD Buffer, Double, 5500W Buffer D.

***Additional experimental data***

The longitudinal gut metagenomes without intervention were used for the comparative data analysis and visualization (Voigt et al., 2015). Also, previously published metagenomes (ENA project ID PRJEB21338) sequenced on the ABI/SOLiD 5500W platform (Boulygina et al., 2017) were used as well as metagenomes (ENA project ID PRJEB18265) sequenced on the Illumina HiSeq 2500 (Gluschenko et al., 2017), and the genomes of *Enterococcus faecium* isolates (NCBI bioproject ID PRJNA412824) (Prianichnikov et al., 2017). Some methods used to manipulate with *E. faecium* isolates are shown in the additional materials (Supplementary Note 2). Summary information on the samples used in the study is available in the Supplementary materials (Supplementary Tables S2-S4).

***Metagenomic sequences data preprocessing***

The metagenomic reads were filtered by quality. Reads with an average quality value (QV) lower than 15 were discarded. To minimize sequencing errors, the remaining reads were processed with SAET software (Life Technologies) with parameters -qvupdate -trustprefix 25 -localrounds 3 -globalrounds 2. Further quality filtration was carried out as following: all positions starting from 5'-end were removed up to the 1st high quality position (QV ≥ 30). After filtering all the reads with the length less than 30 nucleotides were discarded. In order to remove fragments of human DNA from the data, the reads were mapped to the human genome (Homo sapiens GRCh38/hg38) using Bowtie (Langmead et al., 2009) with parameters -f -S -t -v 3 -k 1. If a read could be mapped in two or more places, the reference

was chosen randomly and equiprobable. Reads unmapped to the human genome were converted from the color space to base space and used in further analysis.

***Taxonomic and functional analysis of the metagenomes***

Metagenomic taxonomic and metabolic profiling was performed using HUMAnN2 (Abubucker et al., 2012) (contains MetaPhlAn2 (Truong et al., 2015)) with default parameters (using MetaCyc (Caspi et al., 2007) database for default). Antibiotic resistance (AR) genes were identified in the metagenomes by mapping the reads to MEGARes database (Lakin et al., 2016) using Bowtie with keys -f -S -t -v 3 -k 1. Relative abundance of the group and class AR genes was searched using ResistomeAnalyzer (Lakin et al., 2016) and calculating RPKM (reads per kilobase per million mapped reads) value:

*num reads / ( gene length/1000 * total num reads/1 000 000 ),*

where *num reads* - the number of reads mapped to a gene sequence, *gene length* - length of the gene sequence, *total num reads* - total number of mapped reads of a sample. The number of SNPs in ARGs was obtained by SNPFinder (Lakin et al., 2016). MetaCherchant was applied for the specific metagenomic assembly of the target ARGs context (Olekhnovich et al., 2018). The taxonomic annotation of resulting graph nodes was performed using BLAST.

For each resistance gene (R-genes) to biocides and heavy metals, as well as the virulence factors, homologous genes in the 9.9 mln catalog of human gut microbiota genes (Qin et al., 2010) were determined using BLAST (homology criterion: e-value < $10^{-5}$, percent identity > 80% for > 80% of length) and two databases: BacMet (Pal et al., 2013) and VFDB (Chen et al., 2012). The relative abundance of each template gene was calculated by summing the values of the number of such similar genes from the above-mentioned catalog (according to Dubinkina et al. (2017)). RPKM value was calculated to normalize the mapping data.

Distribution of intraspecies structures in metagenomic data was obtained using ConStrains (Luo et al., 2015) with default parameters. The scale of changes in the relative abundance of intraspecific structures was calculated as a residual of abundances at two time points. The pangenomes of the most abundant bacteria were obtained by PanPhlAn (Scholz et al., 2016) with parameters --left_max 1.5 --right_min 0.5.

***Statistical analysis***

The basic identification of differences at a taxonomic level was performed using linear discriminant analysis effect size (LEfSe) (Segata et al., 2011). The differences between community structures were evaluated using the Bray-Curtis metric. For additional analysis of the metagenomic composition, the MetaFast algorithm based on the adaptive assembly of *de novo* metagenomic reads was used. This algorithm evaluates the differences in metagenomes without the use of taxonomic annotation methods (Ulyantsev et al., 2016). The ADONIS with the Bray-Curtis dissimilarity metric was used to identify the factors affecting the patients microbiota taxonomic composition (Oksanen et al., 2007). Factors included gender, age, duodenal ulcer, chronic duodenitis, chronic gastritis, GERD and time point. The factors which significantly (threshold P<0.1) influenced the microbiota taxonomic composition were added to the multivariate analysis MaAsLin (Morgan et. al., 2012).

Relative abundance of different species and genera were considered as dependent variables. Analysis scheme was as follows:

*relative abundance of genus/species~time point+duodenal ulcer+gender*

Also, LEfSe was used to evaluate the statistical significance of differences in the relative abundances of MetaCyc metabolic pathways with parameters -a 0.05, -w 0.01, -l 3.

To determine the differences in relative abundance of ARGs, R-genes (antibiotics and biocide / metals) and virulence factors the following operation were performed: the differences in the representation profiles were determined using the paired Mann-Whitney test (significance threshold: adjusted P<0.01) then significant differences of features were identified using gene set analysis (GSA) from piano bioconductor package (Väremo et al., 2013) (parameters: gene set analysis using “reporter feature algorithm,” significance assessment using “gene sampling”, gene set significance threshold: adjusted P<0.05 (according to Dubinkina et al. (2017)).

Paired Mann-Whitney test with Benjamini-Hochberg correction for multiple testing (FDR) was used for the additional differential analysis. Data visualization was performed using R (R core team) and GraPhlAn (Asnicar et al., 2015).

## Results

### *Cohorts of patients and available data*

In total, 80 metagenomic samples collected from 40 patients (47.7±13.11 years old, 18 female and 22 male) before and after the *H. pylori* eradication therapy lasting 14 days were examined. The samples obtained were divided into groups to perform statistical analysis. The first group included metagenomes collected prior to the eradication therapy (1st time point, 40 metagenomic samples). The second group included metagenomes from samples collected 0-2 days after taking drugs (2nd time point, 40 metagenomic samples).

The sequencing of the stool samples yielded 30.2±10.0 M of 50 bp reads per sample (120.9 Gbp in total). According to the rarefaction analysis results (Supplementary Figure S1), the obtained number of reads is sufficient to determine a significant part of the taxonomic and functional profile of the patient's microbiota. Summary data on samples and patients are presented in additional data (Supplementary Tables S1).

### *Eradication therapy affects composition and richness of gut microbiota*

As a result of taxonomic profiling with MetaPhlAn2, 51 genus and 106 species were detected in the patients’ metagenomes. Eubacterium (15.46%±%13.45), Bacteroides (14.52%±16.92%) and Prevotella (14.43%±22.37%) were the most abundant genera at the 1st time point. The taxonomic composition of the 2nd point metagenomes was different: the most abundant genera included Bacteroides (22.77%±22.06%), Prevotella (14.06%±23.34%), Eubacterium (10.01%±16.08%). An increased relative abundance of Escherichia and Enterococcus was found after the therapy in the samples collected from four patients. Tables of taxonomic abundances at the genera and species levels are presented in additional materials (Supplementary Tables S5-S6). The GraPhlAn visualization of the patient's gut microbiota community for two time points is presented in the Supplementary Figure S2. The differences in the taxonomic structure of the patient's

intestinal microbiota at two time points according to LEfSe analysis are presented in Figure 1.

We compared the alpha-diversity (the total number of identified microorganisms, the relative abundance threshold is 0.1%) and the Shannon indices between the 1st and the 2nd time points. The alpha-diversity of the intestinal microbiota composition differed significantly between the metagenomes prior to and after the eradication therapy: for the observed species Mann-Whitney $P=2.80\times10^{-5}$, for Jensen-Shannon index P=0.01 (see Supplementary Figure S3). However, there was no clear evidence for difference between the metagenomes of the 1st and 2nd time points based on the taxonomic composition (ANOSIM of Bray-Curtis dissimilarity values, R=0.075, P=0.002, 10 000 permutations). Distribution of the patients' gut community structures compared to the healthy persons at two time points is shown in Figure 2 (Voigt et al., 2015).

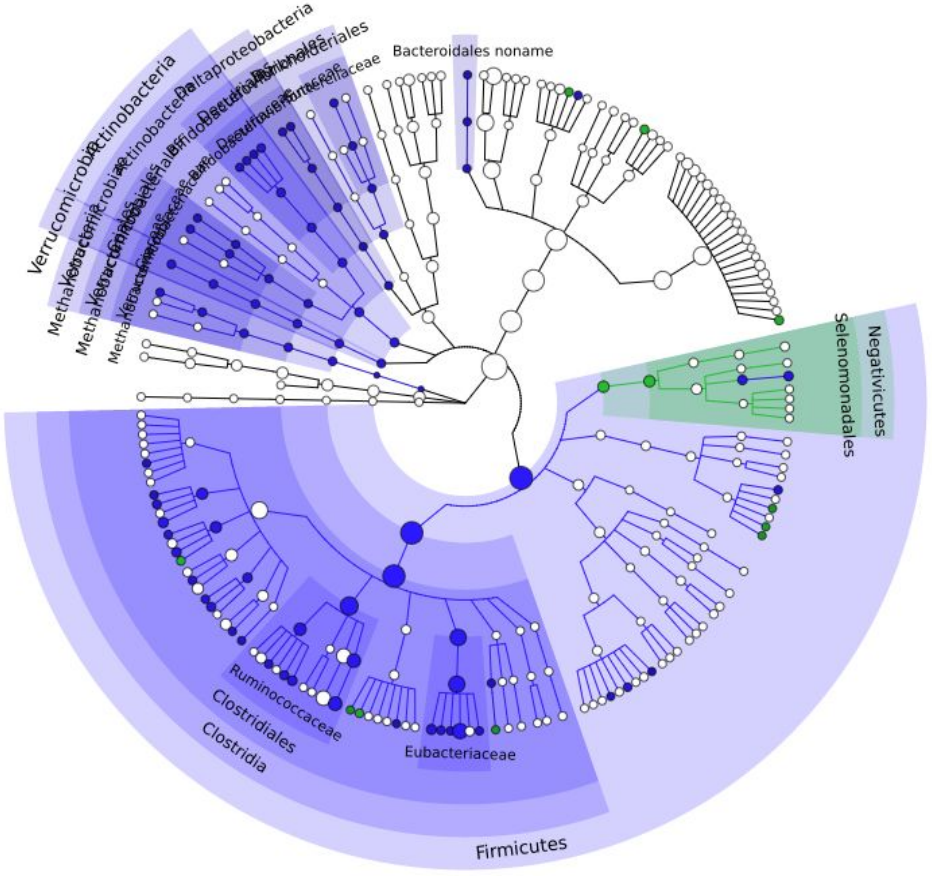


**Figure 1. Differences in intestinal microbiota taxonomic structure before and after *Helicobacter pylori* eradication therapy (based on LEfSe analysis with default parameters).** GraPhlAn cladogram (circular hierarchical tree) of samples grouped by 1st and 2nd time points. Each dot represents bacterial taxon. OTUs significantly increase in 1st time point shown by blue color. Similarly, OTUs significantly increase in 2nd time point denoted by green color. The various shades of colors highlighting the background indicate that the changes consistent at several taxonomic levels.

To visualize the scale of changes in the taxonomic profile, the change in the alpha-diversity (Shannon / Simpson index) and the Bray-Curtis distance between the metagenomes of each patient at the 1st and 2nd time points was plotted (Figure 3). We observed that some metagenomes of the experimental group have undergone moderate (below mean value), medium (above mean value) and severe (higher than mean+SD)

changes, whereas the metagenomes of those individuals who didn't take therapy (Voigt et al., 2015) did not show severe changes in the taxonomic composition on days 7 and 60 and were in the moderate zone. There were statistically significant differences in Bray-Curtis distance between time points in the experimental and control samples: Mann-Whitney P = $2.43 \times 10^{-9}$.

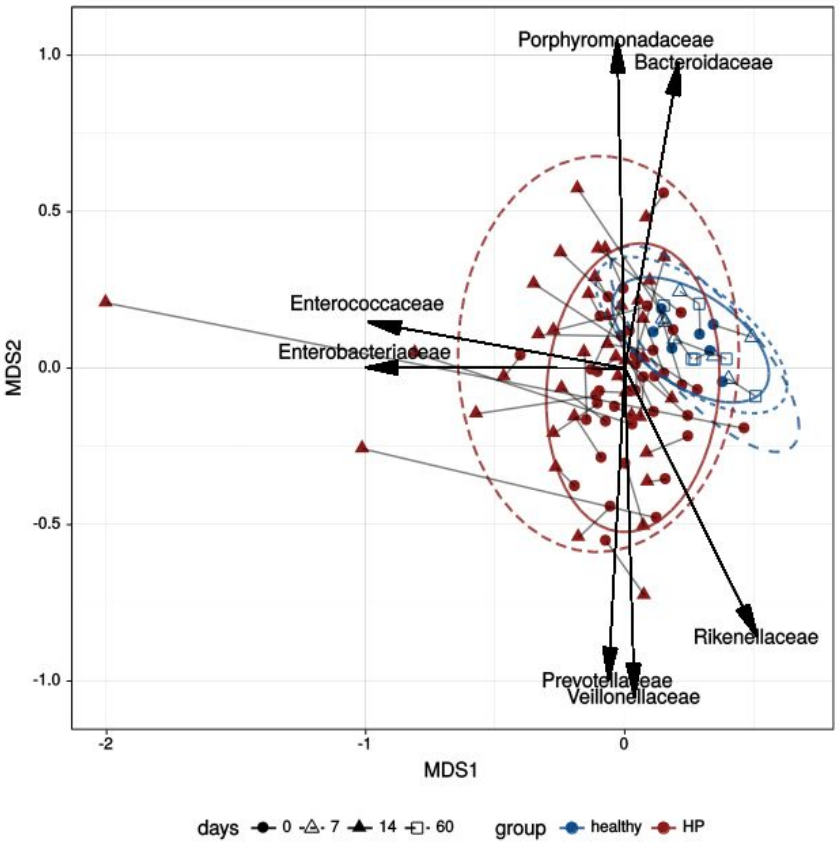


**Figure 2. MDS of gut microbial community structure of the patients prior to and after therapy compared to the microbial community structure changes of the healthy individuals at different time points (Voigt et al., 2015).** Multidimensional scaling (MDS) biplot using Bray-Curtis dissimilarity metric. The labels denote the directions of the increasing abundance of the respective microbial family. Red color denotes patients with *H. pylori* eradication group, blue color refers to the control one. Time points are shown by marks of different shape. The samples collected from the same patient are connected by lines. The components have parameters $P<0.05$, $R^2 >0.15$ according to envfit analysis from the R vegan package (Oksanen et al., 2007).

Conclusions, based on the taxonomic profiles obtained using MetaPhlAn2, were confirmed by MetaFast which is taxonomic-free computational method based on the *de novo* combined adaptive assembly of metagenomic reads (Ulyantsev et al., 2016). The results are shown in the Supplementary Figure S4. Dependence of the metagenomes distance of the 1st time point from the control group and the scale of microbiota changes after eradication therapy were not identified (Spearman R=0.20, P=0.21, see Supplementary Figure S5A). However, the greater the change after the therapy, the farther the 2nd time point from the control group (Spearman R=0.64, $P=1.4\times10^{-5}$, see Supplementary Figure S5B). On the other hand, the scale of changes associated with *H. pylori* eradication therapy may depend on some specific characteristics. The study of the different clinical factors effect on the patient's

intestinal microbiota taxonomic composition is given below. The relative abundances of microbial genera/species are shown in Supplementary File S3.

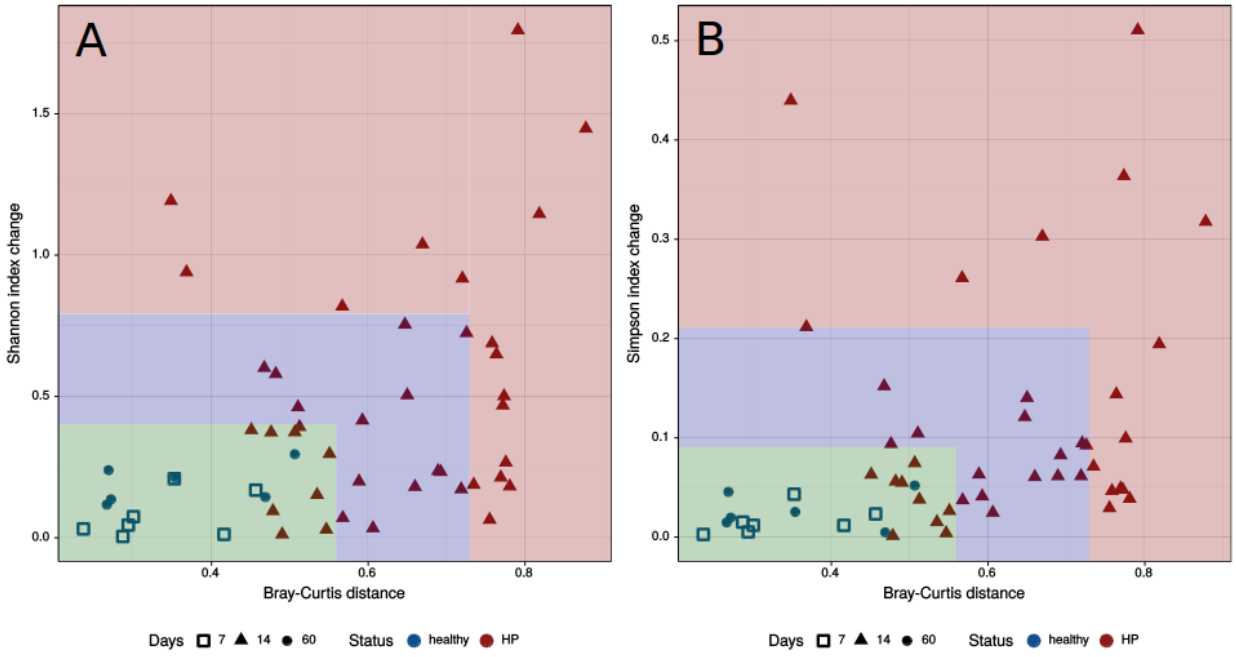


**Figure 3. The scales of changes in the gut microbiota taxonomic composition caused by *H. pylori* eradication therapy.** The X-axis shows the Bray-Curtis distance (**A, B**) between the 1st and 2nd time points. Y-axis denoted the module of difference between the alpha diversity indexes such as Jensen-Shannon (**A**) and Simpson (**B**) of the 1st and 2nd time points. Case group variables are shown as the red dots, the blue dots denote control group variables (Voigt et al., 2015). The green color area show change below mean value (<mean), blue color area - above mean value (>mean, but <mean+SD), variables above mean value are in the red color area (>mean+SD).

***Size of Eradication therapy effect on gut microbiota composition is different depending on disease and gender***

Analysis of variance using distance matrix (ADONIS of Bray-Curtis dissimilarity, 10 000 permutations) was performed to reveal factors which influence microbiota taxonomic composition (ADONIS of Bray-Curtis dissimilarity, 10 000 permutations). According to the obtained results, the most relevant factors shaping microbiota composition are gender ($R^2$=3.97, adj. P=0.0027), time point ($R^2$=3.53, adj. P=0.0036), and duodenal ulcer ($R^2$=2.03, adj. P=0.0836). It should be noted that patients with duodenal ulcer have shown more significant distance change from the 1st time point compared with the rest of the patients (Mann-Whitney P=0.0076). Similar effect was observed in female patients regardless of diagnosis (Mann-Whitney P=0.0050) (see Supplementary Figure S6).

The significant factors revealed were further used in MaAsLin analysis workflow. It was shown that relative abundance decrease of 7 genera and 13 species was associated with eradication therapy treatment (q-value<0.05). The taxa with decreased abundance include Bifidobacterium (*Bifidobacterium adolescentis, Bifidobacterium longum*), Eubacterium (*Eubacterium biforme, Eubacterium ventriosum*), Ruminococcus (*Ruminococcus callidus, Ruminococcus lactaris*), *Roseburia hominis*, *Collinsella aerofaciens*, *Dorea longicatena, Akkermansia muciniphila, Bacteroidales bacterium ph8, Dialister invisus,*

*Coprococcus catus*. Te data are shown in Supplementary Figure S7. For factors gender and duodenal ulcer, changes were determined with 0.25>q-value>0.05.

***Functions of gut microbiota after eradication therapy propensity toward metabolic profile perturbation and increase macrolide resistance potential***

We estimated the functional capacity of patients' gut microbiota in different time points. Following eradication treatment four MetaCyc metabolic pathways associated with carbohydrate and chorismate metabolism were decreased (see Supplementary Tables S7-S8).

To study human gut microbiota functional shift in more detail, we analysed three specific microbiota functions which may be associated with eradication therapy components. Firstly, we studied antibiotic resistance as antibiotic treatment may have influence the distribution of resistance genes in the microbial community (Modi et al., 2014). The second microbial community function under study was resistance to biocide and heavy metals because eradication therapy includes bismuth subsalicylate treatment. As a third characteristic, we considered virulence factors as it has been shown that following antibiotic treatment opportunistic microorganisms get an advantage (Modi et al., 2014).

We have revealed 135 genes groups which determine resistance to 16 antibiotic classes (Supplementary Tables S9). Antibiotic genes abundances increased following eradication therapy (Mann-Whitney P=0.006). Relative abundance of ErmB (23S rRNA methyltransferase) gene associated with macrolide resistance increased significantly (adj. P=0.003). The number of SNPs in the ermB gene have also increased after the therapy (Mann-Whitney P=0.03), which may be a circumstantial evidence of the increase in the number of the microorganisms that possess this gene. At the same time, the functions which determine tetracycline resistance decreased (adj. P=0.019) (see Supplementary Table S10).

Changes in the abundance of the resistance genes to biocide/metals and virulence factors were not detected (Supplementary Tables S11-S12).

***Eradication therapy affects the distribution of intraspecies structures***

To analyze microbiota composition in more detail, i.e. on the intraspecies structure level, we used ConStrains. To detect intraspecies structures, this approach uses SNPs patterns found in the set of universal genes (Luo et al., 2015). Totally, 500 strains (which is the sum of unique strains for each patient) were detected in the experimental group at the 1st and 2nd time points. We identified 371 intraspecies structures (total sum of the unique strains for each healthy individual***)*** that formed a control sample. Intraspecies structure composition before and after treatment have been compared. The data obtained are shown in Figure 4.

It was shown that intraspecies structures of the treatment group are biased to scatter more than those of the control group. Bray-Curtis distance scales between the two groups was found to be significant (Mann-Whitney P=0.01).

We have compared the relative abundance of each intraspecies structure between the treatment and control groups. Only structures with non-zero relative abundance in two time points were included into the analysis. In control group metagenomes sampled following 7 and 60 days after the 1st sample collection were analyzed separately. The data are presented in Supplementary Figure S8. The analysis revealed that intraspecies structures relative abundance in the experimental group are more unstable than that of the control group. We observed several species which relative abundance was almost constant

but strains distribution varied greatly (i.e. *Faecalibacterium prausnitzii*, *Prevotella copri*, *Alistipes putredinis*, *Bacteroides vulgatus, Bacteroides uniformis*).

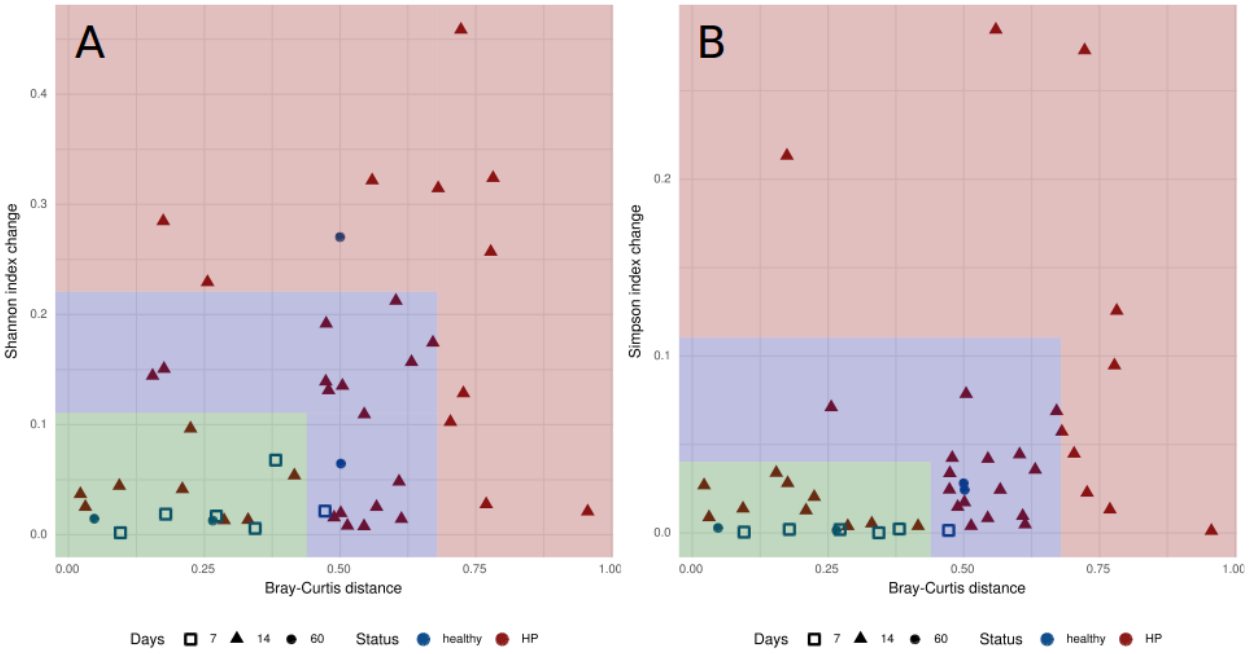


**Figure 4. Intraspecies changes of observed "strains" relative abundance in case and control groups (Voigt et al., 2015).** The X-axis shows the Bray-Curtis distance (**A, B**) between the 1st and 2nd time points. The Y-axis denoted the module of difference between the alpha diversity indexes such as Jensen-Shannon (**A**) and Simpson (**B**) of the 1st and 2nd time points. The variables of case group are shown as the red dots, the blue dots denote control groups. The green color area show change below mean value (<mean), blue color area - above mean value (>mean, but <mean+SD), variables above mean value denoted red color area (>mean+SD).

The PanPhlAn was used to study the functional capacity of specific bacterial species using microbial community data. This strain-level metagenomic profiling tool aims to identify pangenomes of individual strains in metagenomic samples (Scholz et al., 2016). We were able to extract specific genes content from metagenomes for the most abundant taxa in the experimental group. To perform the analysis, these taxa (*Eubacterium rectale*, *Faecalibacterium prausnitzii и Prevotella copri*) were selected and their gene compositions were compared at different time points. Interestingly, changes scale for selected taxa was not the same. Changes of *F. prausnitzii* gene content were found to be more extensive compared with the other two taxa. The results presented in Supplementary Figure S9.

***Eradication therapy affect strains distribution of Enterococcus faecium within microbiota***

*Enterococcus* spp. multiple antibiotics resistance is alarming for the world medical community as this bacterium is prevalent among clinically significant microorganisms. Enterococci may collect different mobile elements and spread antibiotic resistance factors to the broad spectrum of gram-positive and gram-negative bacteria, including the transfer of vancomycin resistance to methicillin-resistant strains of *Staphylococcus aureus* (Lebreton et al., 2017).

We managed to isolate *E. faecium* at two time points from the stool samples of only two patients (HP003, HP010). Strains isolated after the therapy had increased resistance to antibiotics (see Supplementary Table S14), and had higher numbers of ARGs to macrolide and tetracycline antibiotics (ermB, tetL, tetM genes) (Supplementary Figure S10A). Interestingly, *E. faecium strains* isolated after the therapy from both patients were similar in the SNPs pattern, and differed from *E. faecium* strains of the 1st time point (Supplementary Figure S10B). Also, these strains relative abundance in the metagenomes after the therapy has grown when compared to the 1st time point (Supplementary Figure S10C and Supplementary Figure S10D). A more detailed description of the results is given in the supplementary materials (Supplementary Note S3).

***Metagenomic context of the ermB gene shows potential co-localization in genomes of distant bacterial taxa***

To study in more detail the process of acquiring antibiotic resistance growth, the metagenomes of patients (HP003, HP010) were sequenced with Illumina HiSeq 2500. It allows to obtain paired reads of the length sufficient for metagenome assembly. Using MetaCherchant tool (see Materials and methods) we performed the target assembly of the ARGs genomic context. Based on the topology of the obtained graph, we established that the ermB gene was present in *Enterococcus* spp. and *Bacteroides* spp. genomes (Figure 5). The relative abundance of these bacteria increased after the eradication therapy (see Supplementary Figure S11). Also worth noting is the co-localization of the ermB gene, tetL and tetM genes (resistance factors to tetracyclines).

One of the possible scenarios may be that one of the nosocomial strains of *E. faecium* colonized the patient's intestine (because it is identical in the pattern of SNPs in another patient) distributed the mobile element containing the ARG of resistance to macrolides (ermB), which allowed to gain an advantage and grow in the relative abundance during antibacterial therapy the resistance donor himself (*E. faecium*) and recipients - bacteria *Bacteroides dorei* and *Enterococcus faecalis*. On the other hand, the ermB gene could be present in the patient's metagenome before the therapy, but the reads coverage was insufficient to detect its presence (the context of the ermB gene at the 1st time point for patient HP003 was not assembled due to insufficient coverage) and *E. faecium* acted as a recipient of this function. The third possible scenario for the development of events may be the assumption that the genes of ermB *Enterococcus* spp. and *Bacteroides* spp. are independent homologues localized in mobile genetic elements containing homologous sequences.

For the HP010 patient, it was not possible to reconstruct the environment of the ermB gene for any time point due to low coverage.

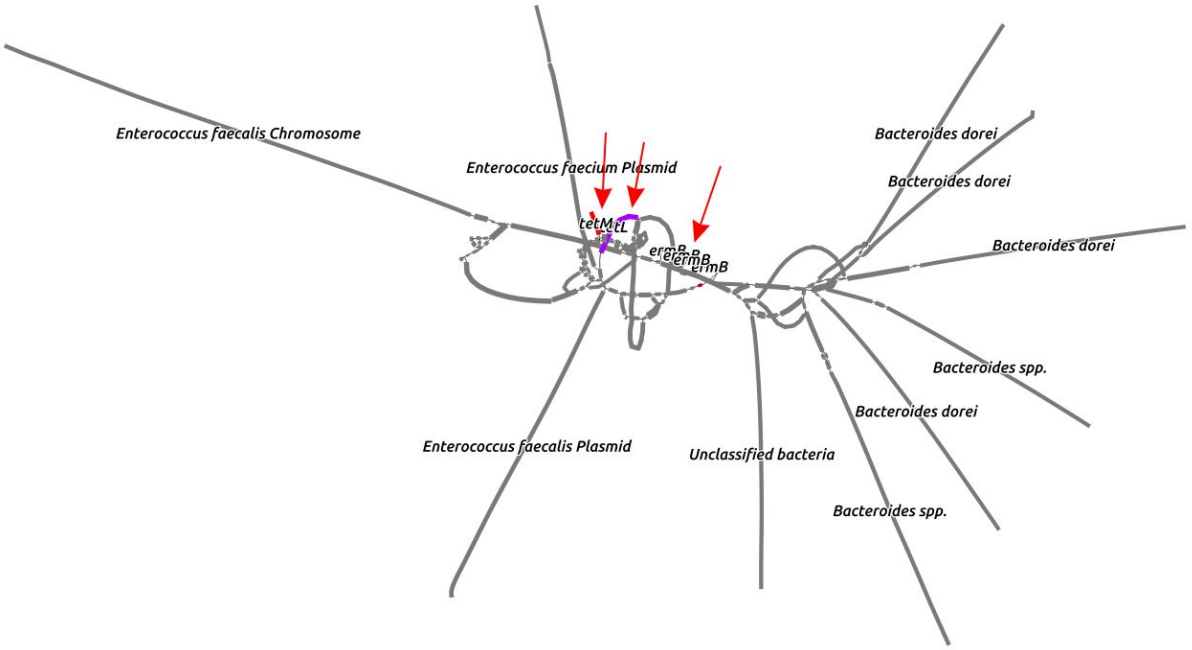


**Figure 5. The graph of ermB gene context obtained by MetaCherchant from HP003 patient (2nd time point) metagenomic data.** The resulting graph showed target gene co-localization with other AR genes - tetL and tetM. ARGs denoted by red arrows. Taxonomic annotation is shown according to the BLAST results.

## Discussion

Changes in the microbial community structure caused by *H.pylori* eradication treatment have been the subject of study before. Yap et al. (2016) used 16S sequencing technique to study microbiota in young adults after eradication treatment. The authors showed that 6 months following the treatment Firmicutes relative abundance decreased, and Bacteroides abundance increased. However, the authors summarize that in general microbial community remains unchanged which may be due to the rather long time period that passed since the treatment and compensatory processes that took place in the microbiota community.

Gut microbial community structure is altered by antibiotic treatment, which was shown both by the results described in this article and the data obtained by other studies (Willmann et al., 2015; Korpela et al., 2016). We showed that eradication therapy decreases the wealth of microbial community. It should be noted that patients with duodenal ulcer and female patients have shown more significant changes in the microbial community taxonomy structure. For female patients, this observation can be explained by a different phase of the menstrual cycle in which samples were taken or by other unknown factors. On the other hand, microbiota of female individuals from the control group didn't show wide shifts within 60 days. It appears that patients with duodenal ulcer showed significant changes due to their reduced condition.

We have revealed taxonomy change biomarkers which appear to be associated with eradication therapy. We observed the decrease in the following bacteria species: *B. adolescentis* and *B. longum* that are involved in the carbohydrate metabolism and prevent

colonization of the gut by opportunistic species (Hütt et al., 2006; Martins et al., 2010); *C. aerofaciens* associated with decreased risk of inflammatory bowel disease (Kassinen et al., 2007); *A. muciniphila* which abundance reduction is thought to be associated with increased weight (Everard et al., 2013; Dao et al., 2015; Plovier et al., 2017). Abundance decrease in some other species, such as *D. longicatena, Bacteroidales bacterium ph8, D. invisus, C. catus, E. biforme, E. ventriosum*, *R. callidus, R. lactaris*, *R. hominis* have also been found. Proton pump inhibitors may cause intrusion of the gut microbiota community by the bacteria species which can't pass gastric acid barrier under normal condition (Jackson et al., 2016; Imhann et al., 2016). However, we didn't reveal any tendency which agrees with this proposition.

We determined statistically significant differences in microbiota functional profiles between the 1st and the 2nd time points. In general, the decline in metabolic pathways associated with complex carbohydrates metabolism was detected: glycogen biosynthesis I (from ADP-D-Glucose), PWY-6737 (starch degradation V) and pathways involved in chorismate synthesis (ARO-PWY and PWY-6163). Perhaps, these changes result from a general impoverishment of the microbial community caused by the eradication therapy. We also detected prevalence tetracycline resistance genes in patients' microbiota before the therapy, which is consistent with previous findings (Hu et al., 2013). However, these genes decreased after therapy. Genes that determine resistance to macrolides (ermB, 23S rRNA methyltransferases group) were found to increase at the second time point. Similar results showing an increase of genes belonging to the 23S rRNA methyltransferases group were reported by Jakobsson et al. (2010).

Microbiota serves as resistance genes reservoir and can transmit these genes to pathogenic bacteria. The decrease in relative abundance of the tetracycline resistance factors is of interest. This effect could be caused by the decline of the bacteria which possess these genes, as tetracycline is not included in the eradication therapy, and presence of the genes which determine resistance to this antibiotic doesn't give the critical advantage to their carriers under given circumstances. Genes which determine resistance to biocide, heavy metals, and also virulence factors remained unchanged.

Interestingly enough, changes of the intraspecies structure distribution were more prominent in the experimental group compared to the control one. We observed perturbations in strains abundances even for those species which abundance were almost constant. This result stresses an importance of strain profiling in metagenomic research as different strains of bacteria can vary significantly in phenotype.

It seems that strains carrying resistance genes, i.e. 23S rRNA methyltransferases, gained an advantage under the strong selective pressure. The *E. faecium* strains isolated from two patients after eradication therapy treatment have shown an increased antibiotic resistance in vitro. These strains had enhanced resistance to macrolides, which is determined by 23S rRNA methyltransferase gene, and possessed virulence factors, such as collagen adhesin protein Scm. In addition, these strains were more abundant after the treatment when compared to the strains isolated at the first time point. These observations are consistent with the findings of the bioinformatics analysis.

Horizontal gene transfer (HGT) could be another possible way which enhances microbiota resistance potential to antibiotics. Using MetaCherchant tool, we constructed the graph structure which contains members of *Enterococcus* and *Bacteroides* spp. and represents metagenomic context of the ermB gene. This graph structure clearly shows that

the target ermB gene is localized in close proximity to the tetracycline resistance genes (tetL and tetM). It can be assumed that these resistance factors can spread together and cause multiple antibiotics resistance by HGT. The result obtained could be a circumstantial evidence of the ermB gene spread within the intestinal microbiota. This finding certainly requires additional verification, but it shows that new computational methods are able to predict such events.

Thus, *H. pylori* eradication therapy causes multiple shifts and alterations of the intestinal microbiota structure and leads to the accumulation of genes which determine resistance to macrolides. Study of antibiotic treatment in terms of its impact upon the human gut microbiota allows shedding light on of the complex processes that cause accumulation and spread of antibiotic resistance. An identification and understanding of these complicated processes may help to constrain antibiotic resistance spread, which is of great importance for human health care.

**Ethics approval and consent to participate**

The study was approved by the ethical committee of the Federal Research Clinical Center of Physical-Chemical Medicine. Before the start of the study, each patient signed an informed consent.

**Acknowledgements**

This study were financially supported by the Russian Scientific Foundation (grant # 15-14-00066).

**Competing interests**

The authors declare that they have no competing interests.

**References**

1. Sanders MK, Peura DA. *Helicobacter pylori*-associated diseases. Current gastroenterology reports. 2002 Nov 1;4(6):448-54.

2. Queiroz DM, Harris PR, Sanderson IR, Windle HJ, Walker MM, Rocha AM, Rocha GA, Carvalho SD, Bittencourt PF, de Castro LP, Villagrán A. Iron status and *Helicobacter pylori* infection in symptomatic children: an international multi-centered study. PLoS One. 2013 Jul 4;8(7):e68833.

3. Buzás GM. Metabolic consequences of *Helicobacter pylori* infection and eradication. World journal of gastroenterology: WJG. 2014 May 14;20(18):5226.

4. Malfertheiner P, Megraud F, O'morain CA, Gisbert JP, Kuipers EJ, Axon AT, Bazzoli F, Gasbarrini A, Atherton J, Graham DY, Hunt R. Management of *Helicobacter pylori* infection - the Maastricht V/Florence consensus report. Gut. 2016 Oct 4:gutjnl-2016.

5. Bartlett JG. Antibiotic-associated diarrhea. New England journal of medicine. 2002 Jan 31;346(5):334-9.

6. Tong JL, Ran ZH, Shen J, Zhang CX, Xiao SD. Meta - analysis: the effect of supplementation with probiotics on eradication rates and adverse events during *Helicobacter pylori* eradication therapy. Alimentary pharmacology & therapeutics. 2007 Jan 1;25(2):155-68.

7. Wright GD. The antibiotic resistome: the nexus of chemical and genetic diversity. Nature Reviews Microbiology. 2007 Mar;5(3):175.

8. Davies J, Davies D. Origins and evolution of antibiotic resistance. Microbiology and molecular biology reviews. 2010 Sep 1;74(3):417-33.
9. Schjørring S, Krogfelt KA. Assessment of bacterial antibiotic resistance transfer in the gut. International journal of microbiology. 2011 Jan 24;2011.
10. Smillie CS, Smith MB, Friedman J, Cordero OX, David LA, Alm EJ. Ecology drives a global network of gene exchange connecting the human microbiome. Nature. 2011 Dec;480(7376):241.
11. Marshall BM, Levy SB. Food animals and antimicrobials: impacts on human health. Clinical microbiology reviews. 2011 Oct 1;24(4):718-33.
12. Forslund K, Sunagawa S, Kultima JR, Mende DR, Arumugam M, Typas A, Bork P. Country-specific antibiotic use practices impact the human gut resistome. Genome research. 2013 Jul 1;23(7):1163-9.
13. Yarygin KS, Kovarsky BA, Bibikova TS, Melnikov DS, Tyakht AV, Alexeev DG. ResistoMap - online visualization of human gut microbiota antibiotic resistome. Bioinformatics. 2017 Mar 14;33(14):2205-6.
14. Jackson MA, Goodrich JK, Maxan ME, Freedberg DE, Abrams JA, Poole AC, Sutter JL, Welter D, Ley RE, Bell JT, Spector TD. Proton pump inhibitors alter the composition of the gut microbiota. Gut. 2015 Dec 30:gutjnl-2015.
15. Imhann F, Bonder MJ, Vila AV, Fu J, Mujagic Z, Vork L, Tigchelaar EF, Jankipersadsing SA, Cenit MC, Harmsen HJ, Dijkstra G. Proton pump inhibitors affect the gut microbiome. Gut. 2016 May 1;65(5):740-8.
16. Tyakht AV, Kostryukova ES, Popenko AS, Belenikin MS, Pavlenko AV, Larin AK, Karpova IY, Selezneva OV, Semashko TA, Ospanova EA, Babenko VV. Human gut microbiota community structures in urban and rural populations in Russia. Nature communications. 2013 Sep 16;4:2469.
17. Voigt AY, Costea PI, Kultima JR, Li SS, Zeller G, Sunagawa S, Bork P. Temporal and technical variability of human gut metagenomes. Genome biology. 2015 Dec;16(1):73.
18. Boulygina EA, Markelova MI, Khusnutdinova DR, Siniagina MN, Malanin SY, Abdulkhakov RA, Abdulkhakov SR, Chernov VM, Grigoryeva TV. Shotgun metagenomic data on the human stool samples to characterize shifts of the gut microbial profile after the *Helicobacter pylori* eradication therapy. Data in brief. 2017 Oct;14:458.
19. Glushchenko OE, Samoilov AE, Olekhnovich EI, Kovarsky BA, Tyakht AV, Pavlenko AV, Babenko VV, Larin AK, Kostryukova ES, Malakhova MV, Ilina EN. Data on gut metagenomes of the patients with *Helicobacter pylori* infection before and after the antibiotic therapy. Data in brief. 2017 Apr 1;11:68-71.
20. Prianichnikov NA, Malakhova MV, Babenko VV, Larin AK, Olekhnovich EI, Starikova EV, Chuvelev DI, Glushchenko OE, Samoilov AE, Manolov AI, Kovarsky BA. Draft genomes of *Enterococcus faecium* strains isolated from human feces before and after eradication therapy against *Helicobacter pylori*. Data in brief. 2018 Feb 28;16:511-4.
21. SAET, T. SAET: SOLiD™ Accuracy Enhancement Tool, http://solidsoftwaretools.com/gf/
22. Langmead B, Trapnell C, Pop M, Salzberg SL. Ultrafast and memory-efficient alignment of short DNA sequences to the human genome. Genome biology. 2009 Mar;10(3):R25.
23. Abubucker S, Segata N, Goll J, Schubert AM, Izard J, Cantarel BL, Rodriguez-Mueller B, Zucker J, Thiagarajan M, Henrissat B, White O. Metabolic reconstruction for metagenomic data and its application to the human microbiome. PLoS computational biology. 2012 Jun 13;8(6):e1002358.

24. Truong DT, Franzosa EA, Tickle TL, Scholz M, Weingart G, Pasolli E, Tett A, Huttenhower C, Segata N. MetaPhlAn2 for enhanced metagenomic taxonomic profiling. Nature methods. 2015 Oct;12(10):902.
25. Caspi R, Foerster H, Fulcher CA, Kaipa P, Krummenacker M, Latendresse M, Paley S, Rhee SY, Shearer AG, Tissier C, Walk TC. The MetaCyc Database of metabolic pathways and enzymes and the BioCyc collection of Pathway/Genome Databases. Nucleic acids research. 2007 Oct 27;36(suppl_1):D623-31.
26. Lakin SM, Dean C, Noyes NR, Dettenwanger A, Ross AS, Doster E, Rovira P, Abdo Z, Jones KL, Ruiz J, Belk KE. MEGARes: an antimicrobial resistance database for high throughput sequencing. Nucleic acids research. 2016 Nov 24;45(D1):D574-80.
27. Olekhnovich EI, Vasilyev AT, Ulyantsev VI, Kostryukova ES, Tyakht AV. MetaCherchant: analyzing genomic context of antibiotic resistance genes in gut microbiota. Bioinformatics. 2017 Oct 28;1:11.
28. Qin J, Li R, Raes J, Arumugam M, Burgdorf KS, Manichanh C, Nielsen T, Pons N, Levenez F, Yamada T, Mende DR. A human gut microbial gene catalogue established by metagenomic sequencing. nature. 2010 Mar;464(7285):59.
29. Pal C, Bengtsson-Palme J, Rensing C, Kristiansson E, Larsson DJ. BacMet: antibacterial biocide and metal resistance genes database. Nucleic acids research. 2013 Dec 3;42(D1):D737-43.
30. Chen L, Xiong Z, Sun L, Yang J, Jin Q. VFDB 2012 update: toward the genetic diversity and molecular evolution of bacterial virulence factors. Nucleic acids research. 2011 Nov 8;40(D1):D641-5.
31. Luo C, Knight R, Siljander H, Knip M, Xavier RJ, Gevers D. ConStrains identifies microbial strains in metagenomic datasets. Nature biotechnology. 2015 Oct;33(10):1045.
32. Scholz M, Ward DV, Pasolli E, Tolio T, Zolfo M, Asnicar F, Truong DT, Tett A, Morrow AL, Segata N. Strain-level microbial epidemiology and population genomics from shotgun metagenomics. Nature methods. 2016 Mar 21;13(5):435.
33. Segata N, Izard J, Waldron L, Gevers D, Miropolsky L, Garrett WS, Huttenhower C. Metagenomic biomarker discovery and explanation. Genome biology. 2011 Jun;12(6):R60.
34. Ulyantsev VI, Kazakov SV, Dubinkina VB, Tyakht AV, Alexeev DG. MetaFast: fast reference-free graph-based comparison of shotgun metagenomic data. Bioinformatics. 2016 Jun 3;32(18):2760-7.
35. Oksanen J, Kindt R, Legendre P, O'Hara B, Stevens MH, Oksanen MJ, Suggests MA. The vegan package. Community ecology package. 2007 Oct 3;10:631-7.
36. Morgan XC, Tickle TL, Sokol H, Gevers D, Devaney KL, Ward DV, Reyes JA, Shah SA, LeLeiko N, Snapper SB, Bousvaros A. Dysfunction of the intestinal microbiome in inflammatory bowel disease and treatment. Genome biology. 2012 Sep;13(9):R79.
37. Dubinkina VB, Tyakht AV, Odintsova VY, Yarygin KS, Kovarsky BA, Pavlenko AV, Ischenko DS, Popenko AS, Alexeev DG, Taraskina AY, Nasyrova RF. Links of gut microbiota composition with alcohol dependence syndrome and alcoholic liver disease. Microbiome. 2017 Dec;5(1):141.
38. Väremo L, Nielsen J, Nookaew I. Enriching the gene set analysis of genome-wide data by incorporating directionality of gene expression and combining statistical hypotheses and methods. Nucleic acids research. 2013 Feb 26;41(8):4378-91.
39. R Development Core Team. R: A Language and Environment for Statistical Computing. Vienna Austria R Found. Stat. Comput. 2008. p. 2673.

40. Asnicar F, Weingart G, Tickle TL, Huttenhower C, Segata N. Compact graphical representation of phylogenetic data and metadata with GraPhlAn. PeerJ. 2015 Jun 18;3:e1029.
41. Modi SR, Collins JJ, Relman DA. Antibiotics and the gut microbiota. The Journal of clinical investigation. 2014 Oct 1;124(10):4212-8.
42. Lebreton F, Manson AL, Saavedra JT, Straub TJ, Earl AM, Gilmore MS. Tracing the enterococci from Paleozoic origins to the hospital. Cell. 2017 May 18;169(5):849-61.
43. Yap TW, Gan HM, Lee YP, Leow AH, Azmi AN, Francois F, Perez-Perez GI, Loke MF, Goh KL, Vadivelu J. *Helicobacter pylori* eradication causes perturbation of the human gut microbiome in young adults. PLoS One. 2016 Mar 18;11(3):e0151893.
44. Willmann M, El-Hadidi M, Huson DH, Schütz M, Weidenmaier C, Autenrieth IB, Peter S. Antibiotic selection pressure determination through sequence-based metagenomics. Antimicrobial agents and chemotherapy. 2015 Dec 1;59(12):7335-45.
45. Korpela K, Salonen A, Virta LJ, Kekkonen RA, Forslund K, Bork P, De Vos WM. Intestinal microbiome is related to lifetime antibiotic use in Finnish pre-school children. Nature communications. 2016 Jan 26;7:ncomms10410.
46. Hütt P, Shchepetova J, Loivukene K, Kullisaar T, Mikelsaar M. Antagonistic activity of probiotic lactobacilli and bifidobacteria against entero - and uropathogens. Journal of Applied Microbiology. 2006 Jun 1;100(6):1324-32.
47. Martins AK, Martins FS, Gomes DA, Elian SD, Vieira AT, Teixeira MM, Cara DC, Nardi RM, Nicoli JR. Evaluation of in vitro antagonism and of in vivo immune modulation and protection against pathogenic experimental challenge of two probiotic strains of *Bifidobacterium animalis* var. *lactis*. Archives of microbiology. 2010 Dec 1;192(12):995-1003.
48. Kassinen A, Krogius-Kurikka L, Mäkivuokko H, Rinttilä T, Paulin L, Corander J, Malinen E, Apajalahti J, Palva A. The fecal microbiota of irritable bowel syndrome patients differs significantly from that of healthy subjects. Gastroenterology. 2007 Jul 1;133(1):24-33.
49. Everard A, Belzer C, Geurts L, Ouwerkerk JP, Druart C, Bindels LB, Guiot Y, Derrien M, Muccioli GG, Delzenne NM, De Vos WM. Cross-talk between *Akkermansia muciniphila* and intestinal epithelium controls diet-induced obesity. Proceedings of the National Academy of Sciences. 2013 May 28;110(22):9066-71.
50. Dao MC, Everard A, Aron-Wisnewsky J, Sokolovska N, Prifti E, Verger EO, Kayser BD, Levenez F, Chilloux J, Hoyles L, Dumas ME. *Akkermansia muciniphila* and improved metabolic health during a dietary intervention in obesity: relationship with gut microbiome richness and ecology. Gut. 2015 May 22:gutjnl-2014.
51. Plovier H, Everard A, Druart C, Depommier C, Van Hul M, Geurts L, Chilloux J, Ottman N, Duparc T, Lichtenstein L, Myridakis A. A purified membrane protein from *Akkermansia muciniphila* or the pasteurized bacterium improves metabolism in obese and diabetic mice. Nature medicine. 2017 Jan;23(1):107.
52. Hu X, Wang T, Jin F. Alzheimer's disease and gut microbiota. Science China Life Sciences. 2016 Oct 1;59(10):1006-23.
53. Jakobsson HE, Jernberg C, Andersson AF, Sjölund-Karlsson M, Jansson JK, Engstrand L. Short-term antibiotic treatment has differing long-term impacts on the human throat and gut microbiome. PloS one. 2010 Mar 24;5(3):e9836.